Available online at www.sciencedirect.com
ScienceDirect
Cement and Concrete Research 36 (2006) 2039–2048
Cement and Concrete Research

Synthesis, characterization and reaction behaviour of lamellar AFm phases with aliphatic sulfonate-anions

Herbert Pöllmann *, Stöber Stefan, Edda Stern

University of Halle, Faculty for Geosciences, Mineralogy/Geochemistry, Von Seckendorffplatz 3, 06120 Halle, Germany

Received 25 July 2005; accepted 23 June 2006

Abstract

The addition of alkanesulfonates as admixtures to cementitious materials allows the formation of new lamellar phases (AFm), which was proofed by X-ray diffraction (XRD). The course of hydration was investigated by heat flow calorimetry.

The layered structures of AFm phases are composed of brucite-like main layers and interlayers containing alkanesulfonate ions and additional H_2O molecules. These structural not necessary H_2O molecules release gradually at definite steps with increasing temperature. With varying relative humidity the layer thickness c' of short aliphatic chained calcium aluminate alkanesulfonate hydrates changes considerably, whereas large organic molecules dominate the layer thickness of those with longer aliphatic chains. By means of the increase of layer thickness with increasing chain lengths it is possible to determine the tilt angles of the aliphatic chains in the interlayers.

Keywords: Calcium aluminate hydrates; AFm phases; Alkanesulfonates; Interlayer; Chain lengths; Tilt angles

1. Introduction

Sulfonates are widely used as admixtures to control and influence the hydration behavior of cementitious mixtures. Usually, only the setting and the rheological behavior of cement pastes are documented, whereas preliminary data on the formation of new phases, which can be formed during the hydration in presence of sulfonates, have been documented [1,2].

Lamellar calcium aluminate ferrate hydrates ($C_4(A,F)H_x$) crystallize during the hydration reactions and belong to the AFm group. AFm-phases form layered structures. The brucite-like main layers $[Ca_2Al(OH)_6]^+$ are described as main layers and interlayers containing anions like OH^- and different amounts of water molecules $[(OH)\cdot nH_2O]^-$ [3–6]. Because AFm phases are based on a layered structure model with sequences of so-called main layers $[Ca_2Al(OH)_6]^+$ and interlayers $[X\cdot nH_2O]-$ X=organic anion, c' describes the distance between two main layers. When the layer distance of two main layers is equal to c_0 (crystallographic lattice constant) then $c_0=c'$. If the translation period c must be elongated due to different stacking of the layers, the stacking sequence is given by: $c_0=n\cdot c'$ (n=integer). The hydroxide ions of the interlayers can be replaced by various inorganic ions, such as Cl^-, Br^-, SO_4^{2-}, CO_3^{2-}, CN^-, OH^-, NO_3^-, CrO_4^{2-}, HBO_3^{2-} or organic ions and molecules; alcohols, carboxylic acid anions, sulfonates [5,7–17,29]. Solid solution series, intermediate compounds and superstructures occur due to different anions and reaction conditions [11,14,18]. The incorporation of the organic anions in the interlayer results directly from precipitation or from interlayer exchange reactions [7,19,20]. Additional incorporation of uncharged molecules in the interlayer is also possible [21,22].

The formation of lamellar calcium aluminate hydrates with organic interlayer anions during hydration of cementitious mixtures in the presence of organic additives was expected and observed [18]. For the application of carboxylates and sulfonates in the building material industry, a better understanding of the hydration reactions and the properties of the carboxylate- and sulfonate-containing hydrates are necessary.

* Corresponding author. Tel.: +49 345 5526110; fax: +49 345 5527365.
E-mail address: Herbert.poellmann@geo.uni-halle.de (H. Pöllmann).

0008-8846/$ - see front matter © 2006 Elsevier Ltd. All rights reserved.
doi:10.1016/j.cemconres.2006.06.008

2. Experimental

2.1. Synthesis of pure AFm phases

The synthesis of $[Ca_2Al(OH)_6]^+$ $[OH{\cdot}nH_2O]^-$ as starting material was performed by using molar mixtures of CA or C_3A (burnt from CaO and γ-Al_2O_3 at 1350 °C) and CaO (decarbonised $CaCO_3$ at 1000 °C for 1 h) at a molar CaO/Al_2O_3 ratio of 4:1 and a water/solid ratio of 10–30 according Eqs. (1) and (2):

$$3CaO \cdot Al_2O_3 + CaO + nH_2O \rightarrow 3CaO \cdot Al_2O_3 \cdot Ca(OH)_2 \cdot 18H_2O + mH_2O \quad (1)$$

$$CaO \cdot Al_2O_3 + 3CaO + nH_2O \rightarrow 3CaO \cdot Al_2O_3 \cdot Ca(OH)_2 \cdot 18H_2O + mH_2O \quad (2)$$

After 4 days of reaction the sodium alkanesulfonate salts were added to obtain interlayer exchange reactions according Eq. (3):

$$3CaO \cdot Al_2O_3 \cdot Ca(OH)_2 \cdot 18H_2O + H_2O + 2NaC_nH_{2n+1}SO_3 \rightarrow 3CaO \cdot Al_2O_3 \cdot Ca(C_nH_{2n+1}SO_3)_2 \cdot nH_2O + 2Na^+_{aq} + H_2O \quad (3)$$

The exchange reactions for these syntheses were performed using sodium salts of sulfonates $NaC_nH_{2n+1}SO_3$ with carbon chains $0<n<16$ (Table 1):

The syntheses of calcium aluminate hydroxide hydrates and calcium aluminate alkanesulfonate hydrates were carried out in a CO_2 free atmosphere using CO_2 free water in order to prevent carbonation. The complete preparatory work was done in a glove box under nitrogen atmosphere. The homogenized materials were placed in sealed polyethylene bottles and mixed with a water/solid ratio between 10 and 30 depending on the solubility of the sodium alkanesulfonate salts. To establish equilibrium conditions the suspensions were shaken continuously at room temperature for 5 to 20 weeks.

2.1.1. Preparation of CEM I pastes containing alkanesulfonic acid anions

8 g of CEM I was placed in polyethylene containers. In each case stoichiometric concentrations of 1 m and 0.25 m methane sulfonic acid and 1 m and 0.25 m 1-propanesulfonic and concentrations were added together with the water at w/c = 0.5 to the samples. After homogenizing cement and the water–admixture solution manually for 2 min, the sample containers were closed in order to prevent dehydration and stored at 25 °C.

After 1.5, 2, 4, 8, 16 and 28 days respectively, approximately 1 g of cement was removed from the PE-bottle, the hydration reaction was stopped by treating the cement paste with acetone and dried subsequently in a desiccator over a saturated $CaCl_2$-solution at 35% r.h. Finally, 0.5 g of each sample was investigated by XRD.

Table 1
Properties and source of sodium alkanesulfonic acids

Chemical composition	
Sodium-1 Pentanesulfonate Monohydrate $C_5H_{11}SO_3Na\ H_2O$	Purum > 98% (Aldridge)
Sodium-1 Hexanesulfonate Monohydrate $C_6H_{13}SO_3Na\ H_2O$	Purum 98% (Aldridge)
Sodium-1 Heptanesulfonate Monohydrate $C_7H_{15}SO_3Na\ H_2O$	Purum > 98% (Aldridge)
Sodium-1 Octanesulfonate Monohydrate $C_8H_{17}SO_3Na\ H_2O$	Puriss > 99% (Aldridge)
Sodium-1 Nonanesulfonate $C_9H_{19}SO_3Na$	Puriss 99% (Aldridge)
Sodium-1 Decanesulfonate $C_{10}H_{21}SO_3Na$	Puriss > 99% (Aldridge)
Sodium-1 Undecanesulfonate $C_{11}H_{23}SO_3Na$	Purum > 98% (Aldridge)
Sodium-1 Dodecanelfonate $C_{12}H_{25}SO_3Na$	Purum > 97% (Aldridge)
Sodium-1 Tetradecanesulfonate $C_{14}H_{29}SO_3Na$	Purum > 97% (Aldridge)
Sodium-1 Hexadecanesulfonate $C_{16}H_{33}SO_3Na$	Purum (Aldridge)

Table 2
Instrumental parameters of different used diffractometers

	Non-ambient temperature and moisture XRD experiments (A)	D 5000 Ambient XRD experiments (B)	D 5000 "Cement paste" (C)
Parameters	Values	Values	Values
2θ range [°]	3–40	3–70	5–30
Step [°]	0.02	0.02	0.03
Time	1–2 s	1–2 s	10 s
Generator	35 kV, 20 mA	40 kV, 35 mA	40 kV, 30 mA
Radiation	Cukα	Cukα	Cukα
Mode	Step-scan	Continuous-scan	Continuous-scan
Slits	Fixed 0.5	Fixed 0.5	Variable V20
Detector	Scintillation	Scintillation	Scintillation

2.1.2. Chemical analysis

The precipitate concentrations of CaO, Al_2O_3 and Na_2O were determined quantitatively by an Inductive Coupled Plasma instrument (ICP/AES) SPEKTROFLAME (SPEKTRO) and with a PLASMAQUANT 110 (CARL-ZEISS JENA GmbH). The instruments were calibrated with single- and multi-element standard solutions. A total carbon analyzer CHN 100 (HERAEUS) was used for the quantitative determination of C and S concentrations.

2.1.3. Thermal analysis (TG/DTA)

With the help of a TG/DTA SDT 2960 (TA INSTRUMENTS), the mass loss of dehydration reactions was determined. 0.2 mg sample was continuously heated up at a rate 2 °C/min up to 400 °C in nitrogen atmosphere. Similar experimental parameters were applied for differential scanning calorimeter measurements (DSC) in order to determine the onset-temperatures of dehydration reactions.

2.1.4. Karl–Fischer titration (KF)

Quantitative H_2O analyses were performed with a Karl–Fischer Instrument "AUTOMAT 633" (METROHM). Approximately 0.01 mg sample was put in a metal sample container, stored in the

Table 3
Phase assemblage of CEM I

C_3S [w.-%]	C_2S [w.-%]	C_3A [w.-%]	"C_4AF" [w.-%]	$CaSO_4\ 2H_2O$ [w.-%]
72.5	9.8	7.5	2.6	3.0

Table 4
Samples investigated by heat-flow calorimetry

Acronyms	Samples
Reference	CEM I+0.5 ml H_2O Reference
CC_1	CEM I+0.5 ml 0.25 m $CH_3SO_3^-$ solution
CC_3	CEM I+0.5 ml 0.25 m $C_3H_7SO_3^-$ solution
CC_5	CEM I+0.5 ml 0.25 m $C_5H_{11}SO_3^-$ solution
CC_6	CEM I+0.5 ml 0.25 m $C_6H_{13}SO_3^-$ solution
CC_7	CEM I+0.5 ml 0.25 m $C_7H_{15}SO_3^-$ solution
CC_8	CEM I+0.5 ml 0.25 m $C_8H_{17}SO_3^-$ solution
CC_9	CEM I+0.5 ml 0.25 m $C_9H_{19}SO_3^-$ solution

KF-furnace (KF-688) and the sample was dehydrated at temperatures 100–300 °C. Consequently, the KF was used in combination with the TG/DTG instrument to proof the water concentration of losses in weight indicated by the TG/DTG plot.

The furnace was purged with dry N_2 thus the dehydrated water in gaseous state was transferred into the titration cell of the KF instrument. Finally, H_2O was determined quantitatively by bipotentiometrical dead-stop titration.

2.1.5. X-ray diffraction (XRD)

Samples at 100% r.h. were investigated applying a SIEMENS diffractometer (A) with a reaction chamber. For experiments at intermediate temperature until 500 °C a temperature camera TTK 450 (PAAR) was chosen. The instrumental parameters are shown in Table 2. Samples were dried at 35% r.h. and were investigated using a SIEMENS D 5000 diffractometer (B). In order to decrease texture effects, caused by the orientation of the platy crystals parallel to the sample holder surface, a special side-loading sample carrier was used. For the determination of phase assemblages and newly in-situ crystallized AFm phases, CEM I pastes were analyzed using a SIEMENS D 5000. 0.5 g of dried cement paste was prepared on a low background silicon sample holder. The instrumental parameters (C) were chosen according to Table 2.

2.1.6. IR-spectroscopy

The IR-spectra of pure calcium aluminum alkenesulfonate hydrate precipitates were carried out on an IR EQUINOX 55 (BRUKER) in the range 400–4000 cm^{-1}. Small amounts of sample were mixed with KBr and pressed at 13.3 mbar to transparent discs with a diameter of 1 cm. This method was used to identify different bondings of organic molecules of the calcium aluminate alkanesulfonate.

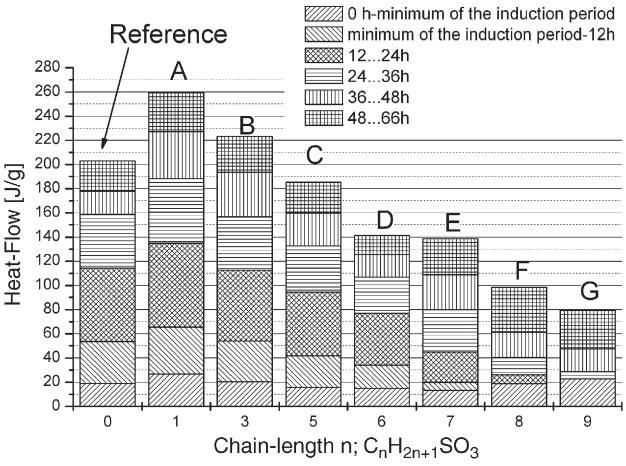

Fig. 2. Integrated heat-flow values of OPC 32,5R+0.25 mol/l $C_nH_{2n+1}SO_3Na$.

2.1.7. Isoperibolic (isothermal) heat-flow calorimetry

The course of hydration of the CEM I (Table 3) was studied under the influence of different alkanesulfonate sodium salts with variable aliphatic chain-length dimensions. The reactions were followed by isoperibolic heat flow calorimetry. The control of temperature is performed by sleeve-control, isothermal calorimeters do have vessel control. The calorimeter construction basics and handling of the instrument can be found in [1,30].

The samples investigated by heat-flow calorimetry are shown in Table 4. 2 g of CEM I was weighed in copper sample containers and closed tightly with a copper cover in order to prevent dehydration of water during cement hydration. 0.25 m alkenesulfonic acid solutions were prepared by solving stoichiometric concentrations of alkanesulfonic acids in H_2O. According to a w/c=0.5, 1 ml solution of each sodium

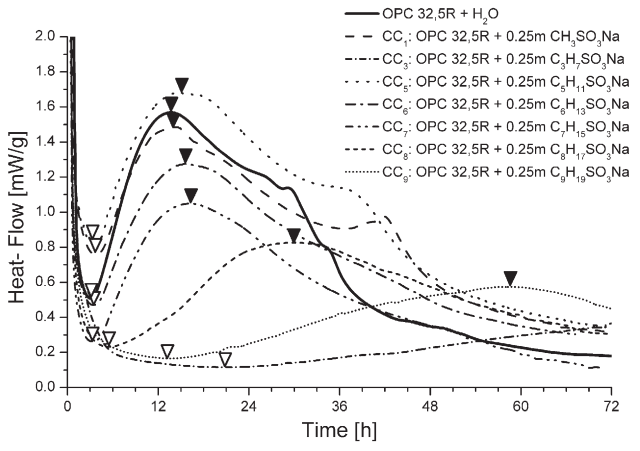

Fig. 1. Heat flow of OPC 32,5R+0.25 mol/l $NaC_nH_{2n+1}SO_3$. Variable chain length of sodium alkanesulfonates.

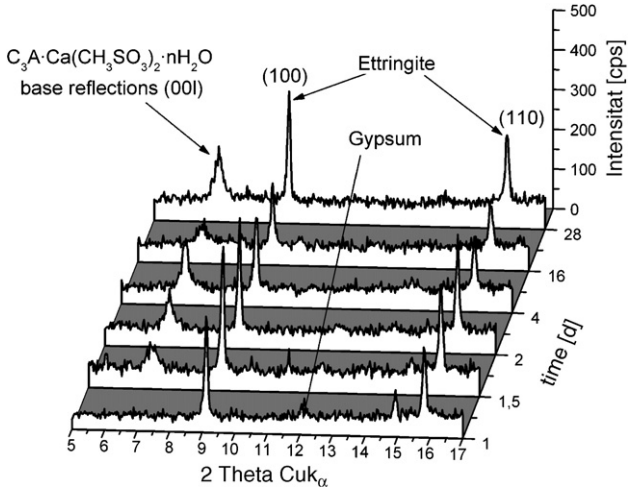

Fig. 3. Phase assemblages in sample A depending on the hydration time.

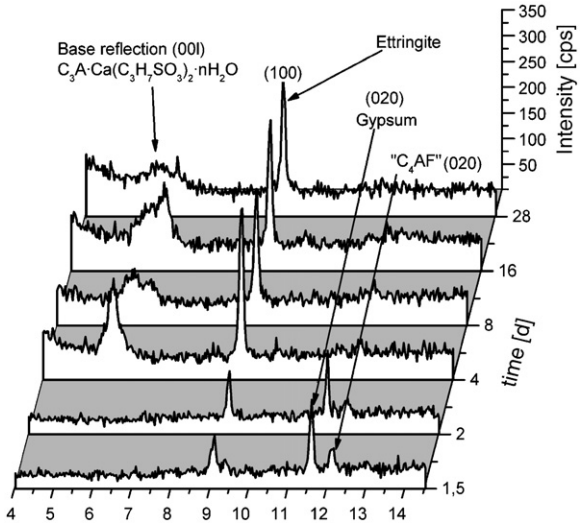

Fig. 4. Phase assemblages in sample B depending on the hydration time.

alkanesulfonic acid salt was put into an injection and stored together with the cement samples in the calorimeter for 24 h. For the experiment, the alkanesulfonic acid solution was injected into the cement sample containers and from this point on the heat-flow [mW/g Cement powder] was recorded 72 h for each sample.

3. Results

3.1. Heat-flow calorimetry

The influence of sodium alkenesulfonic acid solutions on the course of hydration of CEM I is indicated by the time shift (marked with black framed triangles), range of the induction period, the time shift of the main hydration heat-flow maximum (marked with black filled triangles) (Fig. 1) and the integrated heat-flow (Fig. 2).

Fig. 1 demonstrates clearly that the minimum of the induction is shifted to later hydration times due to the addition of sodium alkenesulfonic acid solutions (reference = 3 h, sample CC_9 = 9.9 h, specimen nomenclature is given in Table 4). Furthermore, the duration of the induction periods is expanded drastically especially in the samples CC_7, CC_8 and CC_9. The time shift of the main hydration heat-flow maxima shows the same tendency as the induction period minima. Sample CC_3 and the reference do not show big difference (reference = 13.6 h, sample CC_3 = 13.1 h) but with a stepwise increase of the chain lengths in alkenesulfonic acid anions the main hydration heat-flow maxima are shifted up to 59.0 h (sample CC_8).

The admixture influenced heat-flows distinguish between 2 different groups; CC_1 and CC_2 form group 1 causing an acceleration effect and CC_5, CC_6, CC_7, CC_8 and CC_9 form group 2 causing retarding effects. The criteria for being a member either of group 1 or 2 are the integrated heat-flow during 72 h (Fig. 2). For samples CC_1 and CC_3 higher values were measured compared to the reference. The measured heat-flow values for sample CC_1 are in all sub-time-ranges higher compared to the reference, which indicates an activation of the bulk cement reaction due to the addition of 0.5 ml of a 0.25 m CH_3SO_3-solution. According to Fig. 2 sample CC_3 and the reference produce approximately equal heat-flow quantities up to 36 h, and at higher hydration times the heat-flow of sample CC_3 increases, whereas in Fig. 1 is shown that the heat-flow of sample CC_3 is always smaller during the main hydration and higher values compared to the reference are just detected from 33 h on. The admixtures of group 2 affect particularly the main hydration ("minimum of the induction period" until 36 h). Compared to the reference with a heat-flow of approximately 157 J/g during the main hydration, values of sample CC_5 decreased to 135 J/g, 106 J/g (sample CC_6) and 80 J/g for sample CC_7.

The heat-flow in the range of the main hydration period for sample CC_8 is 27% of the reference sample and the heat-flow for CC_6 is reduced to approximately 15% of the reference.

Based upon the results of the heat-flow experiments, sample CC_1 and CC_3 were investigated by X-ray diffraction (Figs. 3 and 4). In accordance with the XRD scans the crystalline reaction products

Table 5
Cell parameters and layer thicknesses of calcium aluminate hydrates at RT and 100% r.h.

Phase	100% r.h.				35% r.h.			
	a_0 [nm]	c_0 [nm]	n	c′ [nm] (=c/n)	a_0 [nm]	c_0 [nm]	c' [nm]	$\Delta c'$[nm]
$3CaO{\cdot}Al_2O_3{\cdot}Ca(OH)_2{\cdot}18H_2O$	0.577	6.394	6	1.066	0.576	9.505	0.792	0.274
$3CaO{\cdot}Al_2O_3{\cdot}Ca(CH_3SO_3)_2{\cdot}nH_2O$	~0.57	6.561	6	1.094	0.578	7.672	1.279	−0.185
$3CaO{\cdot}Al_2O_3{\cdot}Ca(C_2H_5SO_3)_2{\cdot}nH_2O$	0.575	8.192	6	1.365	0.577	8.130	1.355	0.010
$3CaO{\cdot}Al_2O_3{\cdot}Ca(C_3H_7SO_3)_2{\cdot}nH_2O$	~0.57	9.147	6	1.525	0.576	8.197	1.366	0.159
$3CaO{\cdot}Al_2O_3{\cdot}Ca(C_4H_9SO_3)_2{\cdot}nH_2O$	~0.57	9.480	6	1.580	0.576	9.099	1.517	0.063
$3CaO{\cdot}Al_2O_3{\cdot}Ca(C_5H_{11}SO_3)_2{\cdot}nH_2O$	0.578	10.286	6	1.714	0.575	9.386	1.564	0.150
$3CaO{\cdot}Al_2O_3{\cdot}Ca(C_6H_{13}SO_3)_2{\cdot}nH_2O$	0.578	10.892	6	1.815	0.574	9.676	1.613	0.202
$3CaO{\cdot}Al_2O_3{\cdot}Ca(C_7H_{15}SO_3)_2{\cdot}nH_2O$	0.577	11.568	6	1.928	0.574	10.000	1.667	0.261
$3CaO{\cdot}Al_2O_3{\cdot}Ca(C_8H_{17}SO_3)_2{\cdot}nH_2O$	0.574	11.389	6	1.898	0.575	11.232	1.872	0.026
$3CaO{\cdot}Al_2O_3{\cdot}Ca(C_9H_{19}SO_3)_2{\cdot}nH_2O$	0.575	5.920	3	1.973	0.574	5.832	1.944	0.029
$3CaO{\cdot}Al_2O_3{\cdot}Ca(C_{10}H_{21}O_3S)_2{\cdot}nH_2O$	0.575	12.335	6	2.056	0.575	12.241	2.040	0.016
$3CaO{\cdot}Al_2O_3{\cdot}Ca(C_{11}H_{23}O_3S)_2{\cdot}nH_2O$	~0.57	~12.9	6	2.156	0.575	12.800	2.133	0.023
$3CaO{\cdot}Al_2O_3{\cdot}Ca(C_{12}H_{25}O_3S)_2{\cdot}nH_2O$	0.574	13.324	6	2.221	0.574	13.285	2.214	0.007
$3CaO{\cdot}Al_2O_3{\cdot}Ca(C_{14}H_{29}O_3S)_2{\cdot}nH_2O$	0.576	14.313	6	2.386	0.577	14.292	2.382	0.004
$3CaO{\cdot}Al_2O_3{\cdot}Ca(C_{16}H_{33}O_3S)_2{\cdot}nH_2O$	0.576	15.313	6	2.552	0.575	15.282	2.547	0.005

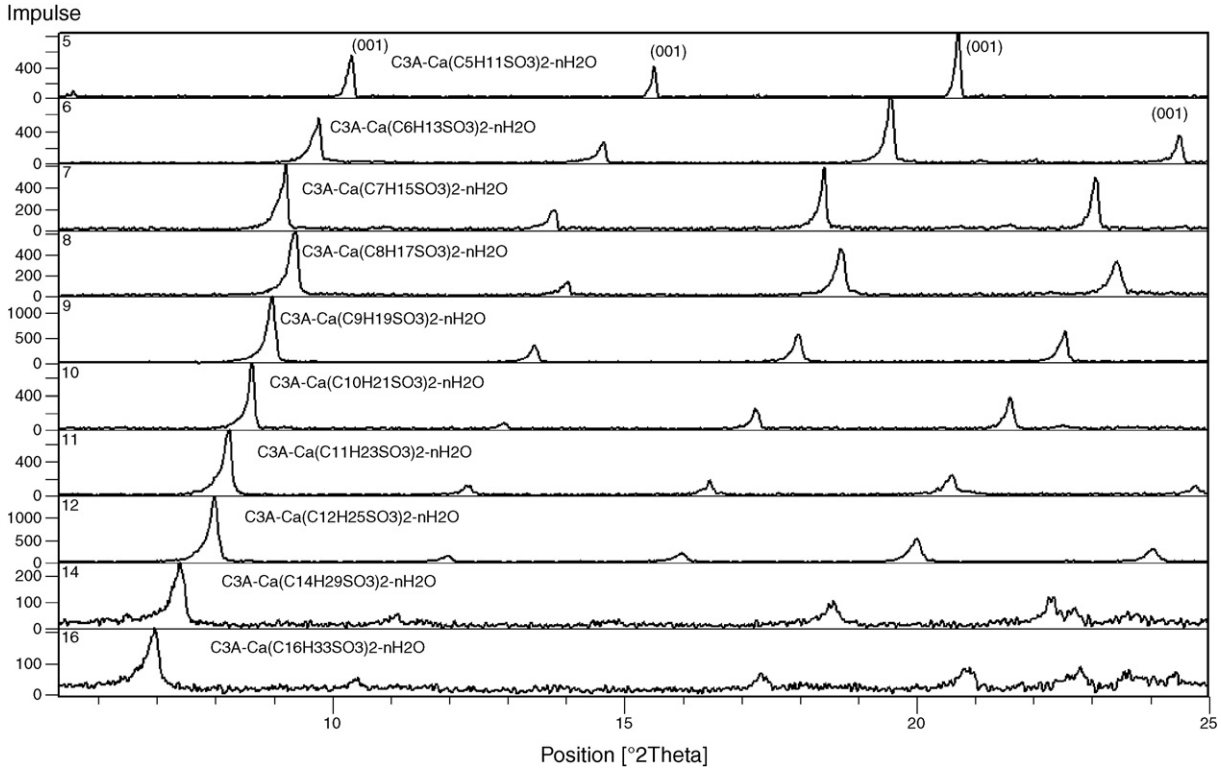

Fig. 5. X-ray diffraction patterns of calcium aluminate alkanesulfonate hydrates at 25 °C and 100% r.h. for $n=5$ to $n=16$.

of the clinker phases, Ettringite (100) and (110) are visible in this section of interest. After 1.5 days (sample CC_1) and 4 days (sample CC_3) previously unknown AFm phases crystallized together with Ettringite, C–S–H phases and Portlandite (not shown in the figures) in both samples. However the "new" AFm phases can only be identified according to (00l)-reflections. In sample CC_1 the peak at approximately 6.9° 2θ (CuK_α) indicate the presence of a *"calcium aluminum methanesulfonate hydrate,"* $C_3A{\cdot}Ca(CH_3SO_3)_2{\cdot}nH_2O$. In sample *based upon the results of* C_3 just one (00l)-reflection was detected at 6–6.5° *based upon the results of* 2θ, indicating a highly distorted and poorly crystalline phase.

These peaks at approximately 6–6.5° 2θ and at 6.9° 2θ cannot be identified as 1.2-nm Monosulfate with (003) at 9.930° 2θ, or to 1.4-nm Monosulfate with (003) at 9.251° 2θ, or Monocarbonate ((001)=11.671° 2θ) or to Hemicarbonate ((006)=10.781° 2θ). These first results motivated the synthesis and characterization of lamellar calcium aluminate alkanesulfonate hydrates.

3.2. Lamellar calcium aluminum alkanesulfonate hydrates

The lattice parameters of the synthesized phases were calculated from XRD data using least-squares refinements. Refinements were performed using initial lattice parameters based on a rhombohedral lattices R with hexagonal axis a_0 and c_0. The layer distances c' calculated for different calcium aluminate alkanesulfonate hydrates at 100% and 35% r.h. are presented in Table 5. For the reaction products of the long-

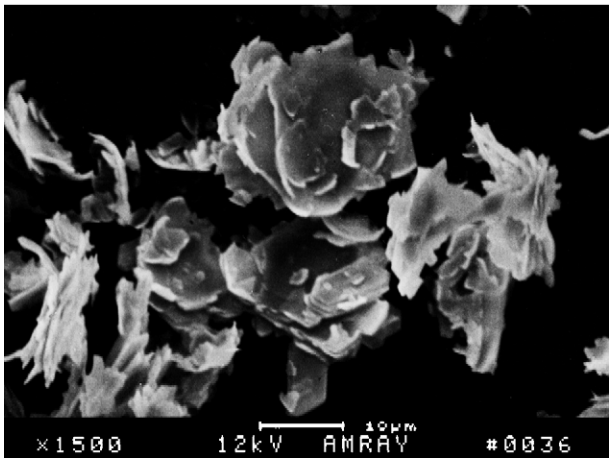

Fig. 6. SEM image of $3CaO{\cdot}Al_2O_3{\cdot}Ca(C_{10}H_{21}O_3S)_2{\cdot}13H_2O$.

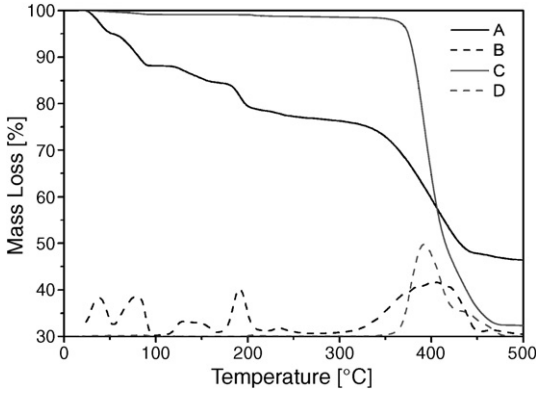

Fig. 7. Thermal analysis TG/DTG of $3CaO{\cdot}Al_2O_3{\cdot}Ca(C_{10}H_{21}O_3S)_2{\cdot}13H_2O$ and $NaC_{10}H_{21}O_3S$ (for comparison), (A) TG of $3CaO{\cdot}Al_2O_3{\cdot}Ca(C_{10}H_{21}O_3S)_2{\cdot}13H_2O$, (B) DTG of $3CaO{\cdot}Al_2O_3{\cdot}Ca(C_{10}H_{21}O_3S)_2{\cdot}13H_2O$, (C) TG of $NaC_{10}H_{21}O_3S$, (D) DTG of $NaC_{10}H_{21}O_3S$.

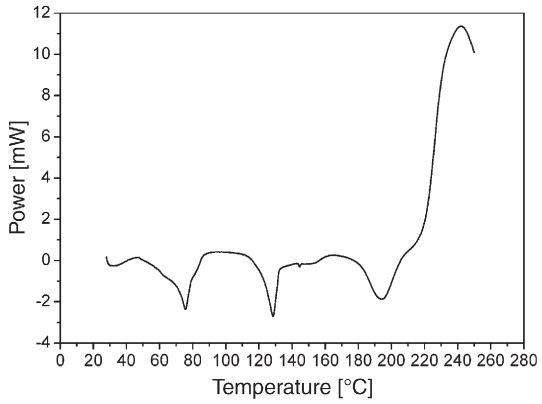

Fig. 8. DSC of $C_3A{\cdot}Ca(C_{10}H_{21}SO_3)_2{\cdot}13H_2O$.

chained sulfonates there is only a slight decrease in the lattice parameters as relative humidity decreases, but there is a considerable decrease in lattice parameters for those with short chains (except for $3CaO{\cdot}Al_2O_3{\cdot}Ca(CH_3SO_3)_2{\cdot}nH_2O$). Peak broadening in some X-ray diagrams indicates layer distortions and also preferential orientation, therefore sometimes only c' (layer thickness) is given.

A comparison of X-ray diffraction patterns of calcium aluminate alkanesulfonate hydrates at 25 °C indicates the shifts of 00l-reflections with increasing chain-length of sulfonates (Fig. 5).

The reaction products always form typical thin layered hexagonal and pseudohexagonal platelets with diameters up to 200 μm. Fig. 6, an SEM-image of $3CaO{\cdot}Al_2O_3{\cdot}Ca(C_{10}H_{21}O_3S)_2{\cdot}13H_2O$ is shown as an example.

3.3. Thermal analysis

Thermal analysis indicates a mass loss in several steps with increasing temperatures (Fig. 7). In each case, Karl–Fischer-measurements carried out at different dehydration temperatures have shown that losses in weight indicated in DSC plots as endothermic reactions were complete dehydration reactions. The thermal behaviour of the different calcium aluminate alkanesulfonate hydrates is comparable concerning temperatures of dehydration and reaction products formed during the process.

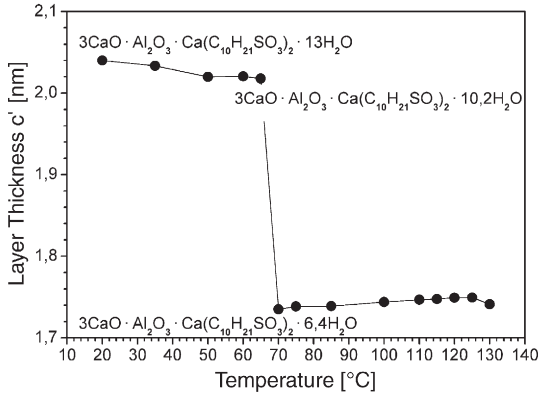

Fig. 9. Layer thickness of $3CaO{\cdot}Al_2O_3{\cdot}Ca(C_{10}H_{21}SO_3)_2{\cdot}13H_2O$ at 35% r.h. with increasing temperature.

Table 6
Thermal stability of the calcium aluminate alkanesulfonate hydrates [18]

Phase	Onset–T stability range [°C]	Basal spacing c' [nm]
$3CaO{\cdot}Al_2O_3{\cdot}Ca(CH_3SO_3)_2{\cdot}16H_2O$	25	1.2787
$3CaO{\cdot}Al_2O_3{\cdot}Ca(CH_3SO_3)_2{\cdot}12H_2O$	31	1.0159
$3CaO{\cdot}Al_2O_3{\cdot}Ca(CH_3SO_3)_2{\cdot}10.5H_2O$	45	0.9243
$3CaO{\cdot}Al_2O_3{\cdot}Ca(CH_3SO_3)_2{\cdot}9H_2O$	72	0.8855
$3CaO{\cdot}Al_2O_3{\cdot}Ca(CH_3SO_3)_2{\cdot}7.5H_2O$	108	–
$3CaO{\cdot}Al_2O_3{\cdot}Ca(CH_3SO_3)_2{\cdot}6H_2O$	176	–
$3CaO{\cdot}Al_2O_3{\cdot}Ca(C_2H_5SO_3)_2{\cdot}15H_2O$	25	1.3549
$3CaO{\cdot}Al_2O_3{\cdot}Ca(C_2H_5SO_3)_2{\cdot}12.5H_2O$	40	1.2134
$3CaO{\cdot}Al_2O_3{\cdot}Ca(C_2H_5SO_3)_2{\cdot}10.5H_2O$	67	–
$3CaO{\cdot}Al_2O_3{\cdot}Ca(C_2H_5SO_3)_2{\cdot}8.5H_2O$	90	–
$3CaO{\cdot}Al_2O_3{\cdot}Ca(C_2H_5SO_3)_2{\cdot}7.5H_2O$	126	–
$3CaO{\cdot}Al_2O_3{\cdot}Ca(C_2H_5SO_3)_2{\cdot}6H_2O$	242	–
$3CaO{\cdot}Al_2O_3{\cdot}Ca(C_3H_7SO_3)_2{\cdot}16H_2O$	25	1.524 and 1.3811
$3CaO{\cdot}Al_2O_3{\cdot}Ca(C_3H_7SO_3)_2{\cdot}14H_2O$	40	1.435
$3CaO{\cdot}Al_2O_3{\cdot}Ca(C_3H_7SO_3)_2{\cdot}12H_2O$	89	–
$3CaO{\cdot}Al_2O_3{\cdot}Ca(C_3H_7SO_3)_2{\cdot}8H_2O$	124	–
$3CaO{\cdot}Al_2O_3{\cdot}Ca(C_3H_7SO_3)_2{\cdot}6H_2O$	204	–
$3CaO{\cdot}Al_2O_3{\cdot}Ca(C_4H_9SO_3)_2{\cdot}16H_2O$	25	1.5165
$3CaO{\cdot}Al_2O_3{\cdot}Ca(C_4H_9SO_3)_2{\cdot}13H_2O$	30	1.4355
$3CaO{\cdot}Al_2O_3{\cdot}Ca(C_4H_9SO_3)_2{\cdot}11.5H_2O$	55	1.3420
$3CaO{\cdot}Al_2O_3{\cdot}Ca(C_4H_9SO_3)_2{\cdot}8.5H_2O$	114	1.3206
$3CaO{\cdot}Al_2O_3{\cdot}Ca(C_4H_9SO_3)_2{\cdot}6H_2O$	250	–
$3CaO{\cdot}Al_2O_3{\cdot}Ca(C_5H_{11}SO_3)_2{\cdot}9.9H_2O$	40–60	1.500±0.002
	65–70	1.448±0.004
$3CaO{\cdot}Al_2O_3{\cdot}Ca(C_5H_{11}SO_3)_2{\cdot}6.4H_2O$	75–135	1.351±0.005
$3CaO{\cdot}Al_2O_3{\cdot}Ca(C_6H_{13}SO_3)_2{\cdot}11H_2O$	20–35	1.612±0.000
$3CaO{\cdot}Al_2O_3{\cdot}Ca(C_6H_{13}SO_3)_2{\cdot}10.5H_2O$	40–70	1.616±0.001
	70–85	1.392±0.002
	90–115	1.426±0.006
$3CaO{\cdot}Al_2O_3{\cdot}Ca(C_6H_{13}SO_3)_2{\cdot}6.6H_2O$	115–125	1.461±0.002
$3CaO{\cdot}Al_2O_3{\cdot}Ca(C_7H_{15}SO_3)_2{\cdot}11H_2O$	25–32	1.667±0.000
$3CaO{\cdot}Al_2O_3{\cdot}Ca(C_7H_{15}SO_3)_2{\cdot}10H_2O$	36–66	1.674±0.005
	66–72	1.724±0.013

Table 6 (*continued*)

Phase	Onset–T stability range [°C]	Basal spacing c' [nm]
$3CaO{\cdot}Al_2O_3{\cdot}$ Ca $(C_7H_{15}SO_3)_2{\cdot}6.3H_2O$	72–125	1.554±0.006
$3CaO{\cdot}Al_2O_3{\cdot}$ Ca $(C_8H_{17}SO_3)_2{\cdot}13H_2O$	20–25	1.874±0.003
$3CaO{\cdot}Al_2O_3{\cdot}$ Ca $(C_8H_{17}SO_3)_2{\cdot}11H_2O$	30–65	1.839±0.007
$3CaO{\cdot}Al_2O_3{\cdot}$ Ca $(C_8H_{17}SO_3)_2{\cdot}7H_2O$	65–120	1.567±0.005
$3CaO{\cdot}Al_2O_3{\cdot}$ Ca $(C_9H_{19}SO_3)_2{\cdot}12H_2O$	21–33	1.946±0.003
$3CaO{\cdot}Al_2O_3{\cdot}$ Ca $(C_9H_{19}SO_3)_2{\cdot}10.8H_2O$	44–65	1.936±0.001
$3CaO{\cdot}Al_2O_3{\cdot}$ Ca $(C_9H_{19}SO_3)_2{\cdot}6.7H_2O$	65–113	1.726±0.004
	117–124	1.786±0.004
$3CaO{\cdot}Al_2O_3{\cdot}$ Ca $(C_{10}H_{21}O_3S)_2{\cdot}13H_2O$	20–35	2.037±0.005
$3CaO{\cdot}Al_2O_3{\cdot}$ Ca $C_{10}H_{21}O_3S)_2{\cdot}10.2H_2O$	50–65	2.019±0.001
$3CaO{\cdot}Al_2O_3{\cdot}$ Ca $(C_{10}H_{21}O_3S)_2{\cdot}6.4H_2O$	70–130	1.743±0.005
$3CaO{\cdot}Al_2O_3{\cdot}$ Ca $(C_{11}H_{23}O_3S)_2{\cdot}11H_2O$	21–37	2.131±0.002
$3CaO{\cdot}Al_2O_3{\cdot}$ Ca $(C_{11}H_{23}O_3S)_2{\cdot}10.1H_2O$	40–67	2.125±0.001
$3CaO{\cdot}Al_2O_3{\cdot}$ Ca $(C_{11}H_{23}O_3S)_2{\cdot}6.3H_2O$	67–120	1.897±0.001
$3CaO{\cdot}Al_2O_3{\cdot}$ Ca $(C_{12}H_{25}O_3S)_2{\cdot}12H_2O$	20–35	2.213±0.002
$3CaO{\cdot}Al_2O_3{\cdot}$ Ca $(C_{12}H_{25}O_3S)_2{\cdot}9.5H_2O$	40–65	2.203±0.002
$3CaO{\cdot}Al_2O_3{\cdot}$ Ca $(C_{12}H_{25}O_3S)_2{\cdot}6H_2O$	65–120	1.912±0.006

In Figs. 7, 8 and 9 the dehydration process was investigated by TG and DSC, and the results of the interlayer variations, measured in combination with high temperature X-ray are given. The compound $3CaO{\cdot}Al_2O_3{\cdot}Ca(C_{10}H_{21}O_3S)_2{\cdot}13H_2O$ is chosen as a representative example.

Mass loss of samples below 120 °C can be interpreted as release of H_2O molecules from the interlayer. The first two steps at temperatures of about 28 °C (±3) and 66 °C (±3) correlate with the decrease of layer thicknesses (Figs. 7 and 9). Above around 120 °C additional water is released. Due to this loss of structurally necessary water, an amorphization of the sample takes place and crystalline AFm phase can no longer be detected by XRD above 130 °C (Fig. 9). At 181 °C and 240 °C additional dehydration reactions of the amorphous AFm-phase were detected by DSC (Fig. 8). The organic components start to decompose at 353 °C by an exothermic reaction (Figs. 7 and 8).

The decrease of c' can be interpreted as shown for the compound $3CaO{\cdot}Al_2O_3{\cdot}Ca(C_{10}H_{21}O_3S)_2{\cdot}13H_2O$ in Fig. 9 with the formation of two new compounds with 10 and 6 water molecules. A comparison of the thermal stability of some selected AFm phases with different alkanesulfonates is given in Table 6.

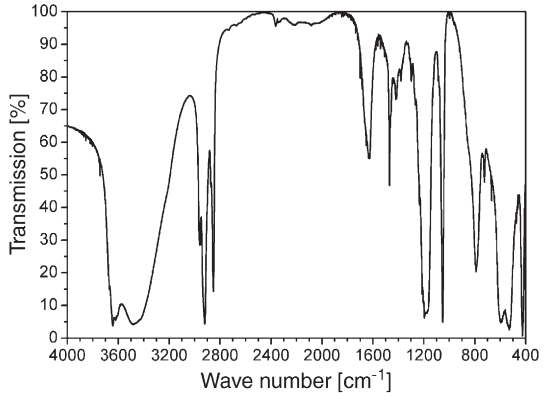

Fig. 10. IR spectrum of $3CaO{\cdot}Al_2O_3{\cdot}Ca(C_{10}H_{21}O_3S)_2{\cdot}13H_2O$.

Table 7
IR-frequencies of $3CaO{\cdot}Al_2O_3{\cdot}Ca(C_{10}H_{21}O_3S)_2{\cdot}13H_2O$

Wave number [1/cm]	Type of vibration
3640–3620	ν(OH)
3480–3450	$\nu_{1,\ 3}(H_2O)$
2960	$\nu_{as}(CH_3)$
2920	$\nu_{as}(CH_2)$
2850	$\nu_s(CH_2,\ CH_3)$
1630	$\nu_2(H_2O)$
1470	$\delta(CH_2)$, $\delta_{as}(CH_3)$
1380	$\delta_s(CH_3)$
1195	$\nu_{as}(SO_3^-)$
1050	$\nu_s(SO_3^-)$
790	ν(C–S), δ(Me-OH)
725	$\rho(CH_2)_n$
595	$\delta_{as}(SO_3^-)$, (AlO_6)
530	$\delta_s(SO_3^-)$, (AlO_6)
425	CaO

3.4. IR-spectroscopy

By means of IR spectroscopy and data from literature it is possible to identify different bonds as well as types of organic molecules in the calcium aluminate alkanesulfonate hydrates [9–11,23–27]. The IR spectra include vibrations of the main layer parts including OH^-, Al–O_6 and Ca–O, vibrations of H_2O molecules in the interlayers, and vibrations of alkanesulfonates like SO_3, CH_2 and CH_3. As an example the IR spectrum for $3CaO{\cdot}Al_2O_3{\cdot}Ca(C_{10}H_{21}O_3S)_2{\cdot}13H_2O$ is given in Fig. 10, and the frequencies are identified in Table 7.

4. Discussion

Systematic variances of the alkanesulfonic acid chain length cause systematic strong influences on the course of hydration of CEM I pastes. The addition of 0.25 m solutions CH_3SO_3H and 1-$C_3H_5SO_3H$ increase the bulk heat-flow measured during 0–72 h. $C_nH_{2n+1}SO_3H$ n=5, 6, 7, 8, 9 affect particularly the cement hydration activity during the main hydration, when C_3S and C_2S react with water. Furthermore, not only the course of hydration is influenced, but also $C_nH_{2n+1}SO_3^-$ n=1, 3 are incorporated in the crystal structure so that different AFm phases incorporating organic acid anions crystallize.

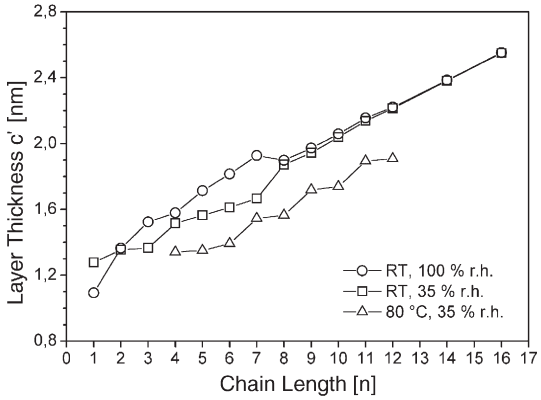

Fig. 11. Layer dimensions of $3CaO{\cdot}Al_2O_3{\cdot}Ca(C_nH_{2n+1}O_3S)_2{\cdot}mH_2O$ with increasing chain length under given conditions.

The layer dimensions of the calcium aluminate alkanesulfonate hydrates investigated at room temperature and 100% r.h. as well as 35% r.h. increase linearly with chain length from $n=4$ to $n=7$ and from $n=8$ to $n=16$ (Fig. 11). For linear increments it is possible to calculate the angles (α) of the alkyl chains tilted to the surface of the hydroxide layers by means of the following empirical formula (Eq. (4)) [7]:

$$\sin\alpha = \Delta c'/0.127 \tag{4}$$

The results of this calculations are given in Table 8. All calculated tilt angles differ from that given in literature for aliphatic monolayers: 90° [13,21,22], 56° [28], 55° [13].

Owing to the knowledge of the tilt angle it is possible to investigate the arrangement in the interlayers and to recalculate the layer thicknesses. The distances in the c direction of the different molecular parts in layered double hydroxides given by several authors [6,28,13] are 0.29 nm for the sulfonate group, 0.18 nm for the C–S bonding, 0.3 nm for the methylene group, 0.2 nm for the hydroxyl groups and 0.31 nm for an additional layer of water molecules (Fig. 12). The application of the following formula (Eq. (5)) modified from Kopka et al. [28] leads to layer thicknesses which differ only slightly from those which were determined from XRD investigations (Table 8):

$$c'_{cal} = 0.29 + 0.18\sin(\alpha + 35°) + (n-1)0.127\sin\alpha + 0.3 + 0.31 + 0.2 \tag{5}$$

with c' expressing the layer distance and n=Carbon atoms composing chain length At 120 °C complete dehydration of the interlayers of calcium aluminate alkanesulfonate hydrates occurs. At 80 °C the increment of the layer thicknesses depends on whether the chains are even or odd numbered (Fig. 12). This may refer to the orientation of the chains in the interlayers [7]. In Fig. 13 for chains of $n=8$–10 the two orientations are shown which produce the lowest and the highest layer thicknesses possible. All other orientations for the same tilt angle will cause thicknesses in between these extremes.

The difference of layer thicknesses between an odd and the following even numbered in Fig. 11 is lower than between an even and the following odd numbered. Therefore the organic chains are oriented in that way to produce the highest thickness possible.

The increment of layer thicknesses of odd numbered chains is nearly the same as that of even numbered chains (Fig. 11). The calculation of the tilt angles by Eq. (4) for odd and even numbered chains leads to 43° on average.

Two different equations are given to calculate the distance A (Fig. 12) for odd and even numbered chains but only for cases the angles are 55° [13]. For other cases the modified equations (Eqs. (6)–(8)) for chains are:

$$A_{odd} = (n-1)0.127\sin\alpha \tag{6}$$

$$A_{even} = (n-2)0.127\sin\alpha + 0.154\sin(\alpha-35°), \text{ for } \alpha > 35° \tag{7}$$

$$A_{even} = (n-2)0.127\sin\alpha, \text{ for } \alpha < 35° \tag{8}$$

within 0.127 nm for the half length of a chain of three C atoms; within 0.154 nm for the absolute distance between two C atoms in a chain.

The results of these equations for tilt angles of 43° in addition to the values for the other components mentioned above except the layer of water leads to layer thicknesses which on average are 0.06 nm below the experimentally obtained values (Table 8).

Table 8
Calculated tilt angles and layer thickness of $3CaO{\cdot}Al_2O_3{\cdot}Ca(C_nH_{2n+1}O_3S)_2{\cdot}mH_2O$ under various conditions

Chain length [n]	Conditions	Tilt angle α [°]	$\varnothing\ c'_{exp}-c'_{cal}$ [nm]	Interlayer H_2O
4–7	RT, 100% r.h.	64.3	−0.033	+
8–16	RT, 100% r.h.	40.1	0.051	+
4–7	RT, 35% r.h.	23.1	0.113	+
8–16	RT, 35% r.h.	42.3	−0.004	+
6–12	80 °C, 35% r.h.	43	0.059	−

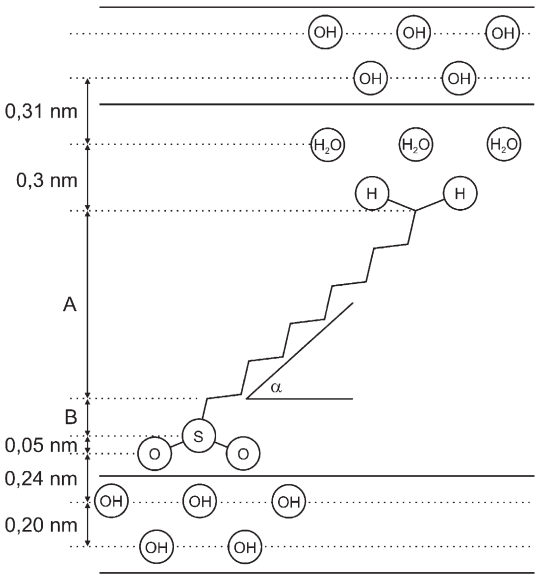

Fig. 12. Calculation of the layer thickness of $3CaO{\cdot}Al_2O_3{\cdot}Ca(C_nH_{2n+1}O_3S)_2{\cdot}mH_2O$; modified from Meyn et al. [13], with $A=(n-1)\ 0.127\sin\alpha$; $B=0.18\sin(\alpha+35°)$.

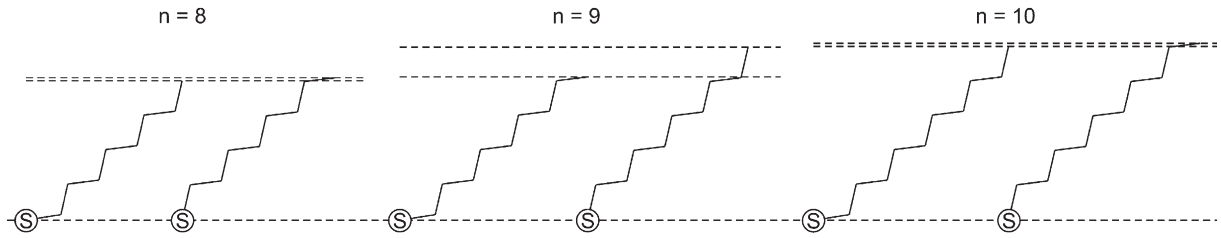

Fig. 13. Possible orientation of alkyl chains with $n=8$, $n=9$ and $n=10$ C atoms for a tilt angle of 43°.

The calculated and measured values for layer thickness are quite similar, despite water contents can influence the layers. The calculations based on these equations give a close look up, but cannot replace precise measurements under real conditions including control of relative humidities to establish definite water contents in the interlayers.

By means of data, equations and models of structure and interlayer arrangements as well [6,7,28,13] and the increments of interlayer thicknesses of the calcium aluminate alkanesulfonate hydrates it is possible to work out some aspects of their interlayer arrangement.

For chain lengths from $n=4$ to $n=7$ the increment of the layer thicknesses at 100% r.h. is different from that at 35% r.h. (Fig. 11). Therefore the calculated tilt angles for the alkanesulfonates in the interlayers differ. The tilt angles decrease from 64° at 100% r.h. to 23° at 35% r.h. (Table 8).

Decreasing basal spacings due to decreasing relative humidity may refer to the release of additional water molecules from the interlayer which either are bound to the organic molecules or pinched in between them [7].

In contrast the layer thicknesses of the calcium aluminate alkanesulfonate hydrates with chain length from $n=8$ to $n=16$ differ only slightly at 100% r.h. and at 35% r.h. Thus the calculated tilt angles vary insignificantly: 40° at 100% r.h. and 42° at 35% r.h. So there is no criterion, which indicates an explicit dehydration reaction caused by decreasing relative humidities for this group of calcium aluminate alkanesulfonate hydrates.

The different behaviour of the calcium aluminate alkanesulfonate hydrates with short chains and long chains may refer to the influence of the polar part, which is greater for alkanesulfonates with short chains. Therefore the interactions in the interlayers and between main layers and interlayers are more distinct.

At 80 °C the water molecules from the interlayers are almost completely released. The increment of the layer thicknesses with increasing chain length is not strictly straight but alternating for chain lengths with $n \geq 6$ depending if the number of carbon atoms is even or odd.

At room temperature; neither at 100% r.h. nor at 35% r.h. the increment of the layer thicknesses depends on if the number of C atoms is even or odd. It is possible that the additional layer of water masks this effect. But this may also refer to the direction in which the chains are tilted. Possibly they are not tilted in that direction the chains are bent as shown in Fig. 12 but perpendicular to that. Especially the tilt angles of 23° calculated for short chains ($n=4$ to $n=7$) in the calcium aluminate alkanesulfonate hydrates indicate orientations like that. In Fig. 13 possible orientation of alkyl chains with $n=8$, $n=9$ and $n=10$ C atoms for a tilt angle of 43 are given. In Fig. 14 three different orientations for alkanesulfonates with chain lengths of $n=5$ and $n=6$ are shown. In case of 14a and 14d the first carbon atoms are beneath the plane of the sulfur atoms. This seems to be improbable. Cases 14c and 14f would lead to same layer thicknesses of their calcium aluminate alkanesulfonate hydrates. But this has not been detected. In cases b and e the chains are tilted perpendicular to the plane opened by the C atoms. Therefore the bends are not visible and definite other parameters can only be seen by direct determination of atomic positions. This seems to be the only way to get constantly increasing layers thicknesses. But this must be proved by further investigation techniques on single crystals.

5. Conclusions

The addition of alkanesulfonates to cement influences the hydration behaviour and can lead to the formation of these AFm phases with aliphatic sulfonate anions. The X-ray data provided can help to identify these new phases. It is strongly recommended to use combinations of methods to clearly identify these phases. It is also highly important to control relative humidity. Shorter chain lengths are more influenced by humidity than longer chain length. Depending on the length of the organic molecule chains of aliphatic sulfonates and the concentrations of the salts acceleration or retardation of hydration of OPC takes place, as demonstrated by heat flow calorimetry.

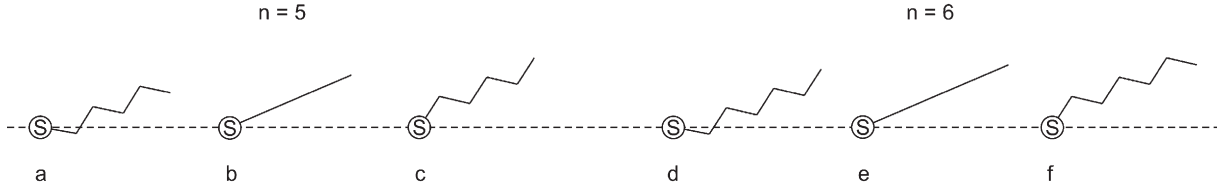

Fig. 14. Possible orientations of alkyl chains with $n=5$ and $n=6$ C atoms for tilt angles of 23°.

Acknowledgements

Part of the work was performed at the Institute for Geology and Mineralogy of the University of Erlangen-Nürnberg to finish doctoral thesis works. Also thanks are due to Prof. Dr. H. Strunk for the possibility of using SEM-facility.

References

[1] H. Pöllmann, S. Stöber, Hydration characteristics and new hydrates using organic additives (carboxylates and sulfonates), 10th ICCC, Göteborg, vol. III, 1997, 3iii032.
[2] V.S. Ramachandran, Concrete Admixtures Handbook: Properties, Science, and Technology, 2. ed., Noyes Publications, Park Ridge, NJ, 1995.
[3] F.G. Buttler, L.S. Dent Glasser, H.F.W. Taylor, Studies on $4CaO{\cdot}Al_2O_3{\cdot}13H_2O$ and the related natural mineral Hydrocalumite, J. Am. Ceram. Soc. 42 (1959) 121–126.
[4] S.J. Ahmed, H.F.W. Taylor, Crystal structure of the lamellar calcium aluminate hydrates, Nature 215 (1967) 622–623.
[5] H.F.W. Taylor, Crystal structure of some double hydroxide minerals, Min. Mag. 39 (1973) 377–389.
[6] R. Allmann, Refinement of the hybrid layer structure $[Ca_2Al(OH)_6]+[1/2SO_4{\cdot}3H_2O]^-$, Neues Jahrb. Mineral., Monatsh. 3 (1977) 136–144.
[7] W. Dosch, Die innerkristalline Sorption von Wasser und organischen Substanzen an Tetracalciumaluminathydrat, Neues Jahrb. Mineral., Monatsh. 106 (1967) 200–239.
[8] H.-J. Kuzel, Beitrag zur Kristallchemie der Calciumaluminathydrate, Habil. Thesis, Frankfurt a. M., Germany, 1969.
[9] C.J.M. Houtepen, H.N. Stein, The enthalpies of formation and of dehydration of some AFm phases with singly charged anions, Cem. Concr. Res. 6 (1976) 651–658.
[10] C.J.M. Houtepen, H.N. Stein, I.R. An, Investigation on some calcium aluminate hydrates, $Ca_2Al(OH)_6+X^-{\cdot}yH_2O$ ($=3CaO{\cdot}Al_2O_3{\cdot}CaX_2{\cdot}nH_2O$, X^- = univalent anion), Spectrochim. Acta 32A (1976) 1409–1414.
[11] R. Fischer, H.-J. Kuzel, Reinvestigation on the system $C_4A{\cdot}nH_2O$–$C_4A{\cdot}CO_2{\cdot}nH_2O$, Cem. Concr. Res. 12 (1982) 517–526.
[12] A. Terzis, S. Filippakis, H.-J. Kuzel, H. Burzlaff, The crystal structure of $Ca_2Al(OH)_6Cl{\cdot}2H_2O$, Z. Kristallogr. 181 (1987) 29–34.
[13] M. Meyn, K. Beneke, G. Lagaly, Anion-exchange reactions of layered double hydroxides, Inorg. Chem. 29 (1990) 5201–5207.
[14] H.-J. Kuzel, H. Pöllmann, Hydration of C_3A in the presence of $Ca(OH)_2$, $CaSO_4{\cdot}2H_2O$ and $CaCO_3$, Cem. Concr. Res. 21 (1991) 885–895.
[15] H. Pöllmann, Carboxylic acid anions: the reaction mechanisms and products with the aluminate phase of cement, 9th ICCC, New Delhi, vol. VI, 1992, pp. 198–204.
[16] S. Auer, H. Pöllmann, Synthesis and characterization of lamellar cadmium aluminium hydroxide salts with SO_4^{2-}, CO_3^{2-}, Cl^- and NO_3^-, J. Solid State Chem. 108 (1994) 1–10.
[17] S. Stöber, H. Pöllmann, Synthesis of a lamellar calcium aluminate hydrate (AFm phase) containing benzenesulfonic acid ions, Cem. Concr. Res. 29 (1999) 1841–1845.
[18] S. Stöber, Einfluβ von Sulfonsäuren und deren Natriumverbindungen auf die Hydratation eines Portlandzementes (CEM I 32,5 R) unter Berücksichtigung der Kristallisation lamellarer Calciumaluminathydrate, Ph D Thesis, Halle (Saale), Germany, 1999.
[19] W. Dosch, H. Keller, H. zur Strassen, Written discussion, 5th ISCC, Tokyo, vol. II, 1968, pp. 72–77.
[20] H. Keller, Anorganische Austauschreaktionen an $[Ca2Al(OH)_6]^+{\cdot}[OH\ aq]^-$ und davon abgeleitete Mischkristallem, Ph D Thesis, Mainz, Germany, 1971.
[21] B. Wang, H. Zhang, D.G. Evans, X. Duan, Surface modification of layered double hydroxides and incorporation of hydrophobic organic compounds, Mater. Chem. Phys. 92 (2005) 190–196.
[22] Y. You, H. Zhao, G.F. Vance, Surfactant-enhanced adsorption of organic compounds by layered double hydroxides, Colloids Surf., A Physicochem. Eng. Asp. 205 (2002) 161–172.
[23] D.O. Hummel, Atlas der Tensidanalyse. FTIR-Spektren und ihre Interpretation, Carl Hanser Verlag, München, Wien, 1996.
[24] M. Hesse, H. Meier, B. Zeeh, Spektroskopische Methoden in der organischen Chemie, Georg Thieme Verlag, Stuttgart, New York, 1987.
[25] K. Nakamoto, Infrared and Raman Spectra of Inorganic and Coordination Compounds, John Wiley & Sons, New York, 1986.
[26] H. Pöllmann, Die Kristallchemie der Neubildungen bei Einwirkung von Schadstoffen auf hydraulische Bindemittel, Ph D Thesis, Erlangen, Germany, 1984.
[27] R. Fischer, Über den Einbau von CO_3^{2-} in laminare Erdalkalialuminathydrate, Ph D Thesis, Erlangen, Germany, 1977.
[28] H. Kopka, K. Beneke, G. Lagaly, Anionic surfactants between double metal hydroxide layers, J. Colloid Interface Sci. 123 (1988) 427–436.
[29] Syntheses, properties and solid solution of ternary lamellar calcium aluminate hydroxi salts (AFm-phases) containing sulfate, carbonate and hydroxide, Neues Jahrb. Mineral., Monatsh. 182/2 (2006) 173–181.
[30] H. Pöllmann, H.-J. Kuzel, H.W. Meyer, Heat-flow calorimetry in cement chemistry — construction and application of a low cost high-sensitive calorimeter, Proc. of the 13th Int. Conf. on Cement Microscopy, Tampa, USA, 1991, pp. 254–272.